

# Analytical Synthesis of Dispersive Mantle Cloaks for Metallic Cylinders: a Zero Contrast Methodology

Giuseppe Labate, Symon Podilchak, Ladislau Matekovits

**Abstract**—In this paper, the problem of reducing the scattering from metallic objects with dispersive surface impedance  $Z_s$  cloaks is addressed. With respect to the literature, where both analysis and synthesis process of cylindrical cloaks are usually solved by classical Mie theory with electric and magnetic fields (E-H) scattering model, an alternative procedure is here suggested for the synthesis of  $Z_s$  coatings, based on the voltage-current (V-I) radial transmission line theory. A unique compact analytical solution for  $Z_s(\omega, m)$  is found in a straightforward manner as a function of the angular frequency  $\omega$  (dispersive behaviour) and the harmonic index  $m$  (scattering mode to suppress) at any frequency regime. In the quasi-static regime, mantle cloaking is obtained as a particular case for  $m = 0$  and, beyond the quasi-static limit, several dispersive functions  $Z_s(\omega)$  can be build by choosing the dominant harmonic index  $m$  with proper dispersion. Without any approximation, the cloaking effect for modes with  $m \geq 0$  is synthesized and validated.

**Index Terms**—Cloaking, Metasurfaces, Radial Transmission Lines, Surface Impedance Cloak.

## I. INTRODUCTION: SCATTERING MODELS FOR CLOAKING

The challenge of creating devices for electromagnetic invisibility and cloaking has fascinated the scientific community with increasing research efforts: from finding plasmonic covers [1] and metamaterial shells [2],[3] to the use of classical impedance models for patterned metasurfaces [4],[5] or transmission line-based cloaks [6], [7]. The robust mathematical theory based on Transformation Optics (TO) [2],[3] has been derived considering the coordinate transformation of a background scenario (by construction, not perturbing fields) into another curvilinear coordinate system supporting the same non-scattering phenomenon, thus discovering unexpected reflectionless systems. For the harmonic suppression of a general scattering event, Scattering Cancellation (SC) has been developed considering Plasmonic Cloaking with bulk metamaterials [1] and Mantle Cloaking with thin metasurfaces [4], [5].

In the present paper, we introduce an alternative methodology for the synthesis of cloaking device based not directly on electric and magnetic fields (E-H) scattering model, as in SC approach [1], [4], but on a voltage-current (V-I) transmission line theory: this choice is demonstrated

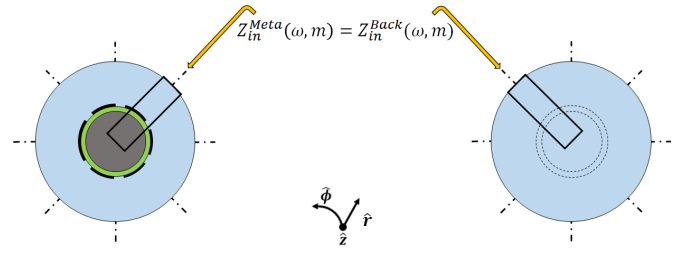


Fig. 1. Cylindrical geometry (top view) with attached coordinate system (center): complete background system (ideal solution of a cloaking problem) with input impedance  $Z_{in}^{Back}(\omega, m)$  (right) and a composite metasurface, made up of ground plane (grey), dielectric cover (green) and loading surface (dashed black line), with input impedance  $Z_{in}^{Meta}(\omega, m)$  (left).

to be more suitable when a surface impedance boundary condition ( $Z_s$ ) is involved in the scattering phenomenon.

In the literature, Mie Theory is a very well assessed technique (e.g., [8]) for the analysis of scattering from rotational-symmetric structures, whereas the synthesis counterpart remains challenging when controlling the zeros of the scattering outside the domain where the device is localized: as the same authors admit in [9], even approximate formulas for different polarizations become cumbersome while still referring to a limited frequency band of application, namely the quasi-static regime [4], [5], [9].

In this paper, the starting equation for imposing such cloaking condition is based on a trivial consideration, as first generalized in [10] and also related to the classical Kirchhoff Current Law and circuit theory [11]: it is illustrated in Fig. 1, namely a *zero contrast methodology*. A conformal metasurface, made up of a ground plane, dielectric substrate and metallic loading (right) can behave as the same geometry but completely filled by background material (left): this equality can be imposed on the input impedance of the cloaked and the complete background device for one (or more) angular frequency value(s)  $\omega$  and one (or more) harmonic mode(s)  $m$  (if the incoming wave is seen as a superposition of independent incoming harmonic waves). It is also worthwhile to mention that the input impedance of conformal structures is non-trivial when formulated in the near-field even for complete homogeneous backgrounds [12], [13].

In the following, the case study will be reducing the scattering from a metallic circular cylinder with a proper surface impedance function  $Z_s(\omega, m)$ . In Section II, the zero contrast methodology is fully developed, step by step, with our new radial transmission line design, extrapolating the surface impedance  $Z_s$  (or admittance  $Y_s$ ) as a function of the  $\omega$  dispersion and harmonic index  $m$ . In Section III, the function  $Z_s(\omega, m)$  is analyzed with Mie Theory and tested in terms of Foster dispersion [14]: as a confirmation, the dispersive function  $Z_s(\omega, m)$  gives mantle cloaking [9] in the quasi-static regime for  $m = 0$ , with improvements on scattering reduction when the size of the metallic cylinder increases. In Section IV, results are

G. Labate is with the Department of Electronics and Telecommunications, Politecnico di Torino, Corso Duca degli Abruzzi 24, I-10129 Torino, Italy (e-mail: giuseppe.labate@polito.it).

S. Podilchak is with the Institute of Sensors, Signals and Systems, Heriot-Watt University, Edinburgh Campus, EH14 4AS, United Kingdom (e-mail: skp@ieee.org).

L. Matekovits is with the Department of Electronics and Telecommunications, Politecnico di Torino, Corso Duca degli Abruzzi 24, I-10129 Torino, Italy and with the Macquarie University, Sydney 2109, NSW, Australia (e-mail: ladislau.matekovits@polito.it).

obtained beyond the quasi-static regime, indicating two possible design strategies for a full dispersive function  $Z_s(\omega)$  as obtained from  $Z_s(\omega, m)$  considering or not Foster dispersion issue, paving the way for the design of passive or active mantle cloaks. In the final section, conclusions and further extension of this work, based on smoothly varying passive impedance metasurfaces [15], radial impedance modeling and control in leaky wave antennas [16] and active metasurface cloaks [17] are indicated.

## II. ANALYTICAL SYNTHESIS OF $Z_s(\omega, m)$ VIA RADIAL TRANSMISSION LINE THEORY

The case study will be cloaking a cylindrical metallic object with a circular cross section, using the cylindrical co-ordinate system  $(r, \phi, z)$ : in this geometry, the propagation of the (incident and scattered) energy happens through a radial direction (i.e., the wavenumber is  $k \equiv |k|\hat{r}$ ) and, as a consequence, through cross sections  $A_r$  that are similar, but non-uniform, because of the radial variance along the structure while traveling, forming  $dA_r(r) = r dr d\phi$ .

To the authors' best knowledge, the first scholar who studied radial lines applied to cloaking problems was Sureau in 1967, but only for pure homogeneous dielectric cloaks [13]. With respect to Sureau's pioneering work, the novelty of the present paper resides in the introduction of an additional lumped surface impedance, with the clear advantage of *tunability* for the cloaking effect, not possible with only a bulk volumetric dielectric cover [13].

The intrinsic anisotropy introduced by such non-uniform cross sections alters completely the V-I algebra with respect to classical uniform transmission lines: the same piece of radial line has different input impedances if computed looking towards the direction of increasing radius (plus sign counting) or decreasing radius (negative sign counting) and the concept of wavelength becomes meaningless, due to this non-uniform cross section variation [12]. Even if different from classical uniform transmission lines (i.e., with constant cross sections), the radial formalism is able to take into account the E or H polarization of the incident wave by considering the respective voltage  $V$  and current  $I$  excited. For example, considering  $\hat{z}$  to be parallel to the cylinder's axis, the V-I waves along the radial line for the  $\text{TM}_z$  polarization are [12]

$$V(r) = V^+ H_m^{(2)}(kr) + V^- H_m^{(1)}(kr) \quad (1)$$

$$I(r) = -jY_B \left[ V^+ H_{m+1}^{(2)}(kr) + V^- H_{m+1}^{(1)}(kr) \right] \quad (2)$$

where  $k$  is the wavenumber in the considered layer (as stressed above, tacitly assumed to be directed along  $\hat{r}$ ),  $Y_B$  is the background intrinsic admittance (i.e.,  $Y_B = \sqrt{\epsilon_b/\mu_b}$ ), whereas  $H_m^{(1)}(\cdot)$  and  $H_m^{(2)}(\cdot)$  are ingoing and outgoing traveling waves. In usual uniform transmission lines, these are plane waves modeled as complex exponential functions, but here they are cylindrical waves modeled as Hankel functions of the first (inward) and second kind (outward) of order  $m$  (or  $m+1$  for the current). For all the particular harmonic modes, the outgoing (or ingoing)

travel is given by the increasing (or decreasing) radius direction [12].

In the following treatment, complete computations will be performed only for the  $\text{TM}_z$  polarization case, which corresponds to the so called  $E$ -type mode for the V-I model [12]: for the  $\text{TE}_z$  case, the  $H$ -type mode description for the V-I model can be simply obtained by duality (i.e., exchanging voltage, current and impedance with current, voltage and admittance, respectively [12]).

Once defined the algebra of non-uniform transmission lines, it is possible to compute, as reported in Fig. 2, the input impedances of two different radial lines: one (left) completely filled by background material and another one (right) modeling a metallic cylinder of radius  $a$ , coated by a ring of dielectric material with permittivity  $\epsilon_r$  and radius  $a < r < b$ , loaded by an unknown surface impedance  $Z_s$  at  $r = b$ .

Embedded in the same background material, if these two structures are equivalent when looking at them from the outward region  $r \geq b$  (i.e., input impedance), a cancellation effect takes place for the  $m^{\text{th}}$  harmonic [13]: here, with the use of a surface impedance, the mathematical residual needed by each scattering  $m$ -wave is automatically adjusted by  $Z_s$ , correcting the volumetric effects only due to the dielectric cover. For the two radial lines in Fig. 2, it is more appropriate to solve for the admittances  $Y$  (and after inverting  $Y_s$  for obtaining  $Z_s$ ), due to the their parallel connection: along the radial direction at the input terminals, located at  $b$ , the zero contrast equation is

$$\chi_Y(\omega) \equiv \tilde{Y}(\omega, r) - \tilde{Y}_b(\omega, r) = 0 \quad \text{at } r = b \quad (3)$$

where both input admittances  $\tilde{Y}$  (cloaked cylinder) and  $\tilde{Y}_b$  (background cylinder) are normalized with respect to the background intrinsic admittance  $Y_B$ .

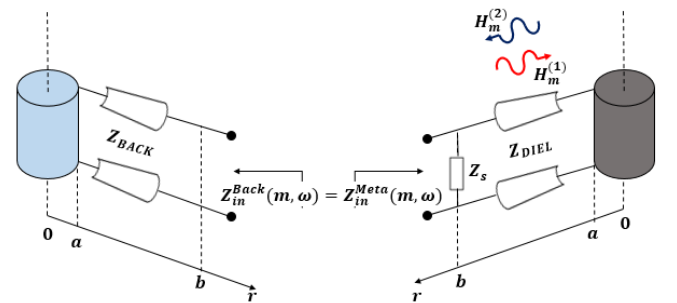


Fig. 2. The complete homogeneous background (left) and a composite metasurface (right) seen as a radial line: zero contrast between  $Z_{in}^{Back}$  and  $Z_{in}^{Meta}$  as a function of  $m$  and  $\omega$ .

As depicted in Fig. 2 (left), the input admittance  $\tilde{Y}_b$  is just the input admittance obtained from a complete background (e.g., free-space) modeled as a radial line: according to the radial line algebra [12], [13], its value is

$$\tilde{Y}_b \equiv \frac{Y_b(\omega, r)}{Y_B} \Big|_{r=b} = -j \frac{J'_m(k_0 r)}{J_m(k_0 r)} \Big|_{r=b} \quad (4)$$

The evaluation of the first derivative (denoted by  $'$ ) is here analytically computed according to one of the several recurrence formulas as reported in [18].

As in classical uniform transmission lines, all computations are performed with normalized values of admittance (or impedance), here the background is always assumed to be free-space. The value  $Y_0$  represents the inverse of the intrinsic impedance in free-space  $Z_0 \equiv 120\pi \Omega$  and  $k_0$  is the free-space wavenumber. As depicted in Fig. 2 (right), the input admittance  $\tilde{Y}$  (cloaked device) contains two contributions: a term  $\tilde{Y}_d$ , obtained by looking at the short circuit (i.e., metal object) through the dielectric radial line and the term  $\tilde{Y}_s$ , representing the loading surface on top of the dielectric coating at  $r = b$  (our design variable).

Due to the voltage reflection coefficient at  $r = a$  (i.e., metallic boundary) being

$$\Gamma^V(r = a) \equiv \frac{V^-}{V^+} \frac{H_m^{(1)}(kr)}{H_m^{(2)}(kr)} \Big|_{r=a} = -1 \quad (5)$$

the ratio  $\gamma^V(\cdot)$  between reflected  $V^-$  and transmitted voltage  $V^+$  at  $a$  is obtained as

$$\gamma^V(ka) \equiv \frac{V^-}{V^+} = -\frac{H_m^{(2)}(ka)}{H_m^{(1)}(ka)} \quad (6)$$

It is worthwhile mentioning that now the wavevector, imposed at the boundary by the presence of the dielectric cover, is  $k = \sqrt{\varepsilon_r} k_0$ . As in classical transmission lines, dividing eq. (2) by eq. (1), it is possible to obtain the admittance through the radial line as a function of the ratio  $\gamma^V(\cdot)$ , as imposed by the specific boundary condition, i.e.,

$$\tilde{Y}_d \equiv \frac{Y_d}{Y_B} \Big|_{r=b^-} = -j \left[ \frac{H_{m+1}^{(2)}(kb) + \gamma^V(ka) H_{m+1}^{(1)}(kb)}{H_m^{(2)}(kb) + \gamma^V(ka) H_m^{(1)}(kb)} \right] \quad (7)$$

Since the input admittance  $Y$  is seen from a free-space region, there is an amplified factor  $\sqrt{\varepsilon_r}$  in front of eq. (7), in order to pass from  $r = b^-$  at  $r = b^+$  [13], where also the surface admittance  $Y_s$  is located in a parallel fashion (i.e., considered to lie above the dielectric substrate, thus in free-space). In a straightforward manner, the unknown admittance  $Y_s$  can be written in a compact form, substituting eq. (4) and Eq. (7) in eq. (3), thus solving for  $Y_s$  obtaining

$$\begin{aligned} \tilde{Y}_s \equiv \frac{Y_s}{Y_B} \Big|_{r=b^+} &= \frac{Y_b - Y_d}{Y_B} \Big|_{r=b^+} = \\ &= -j \frac{J'_m(k_0 b)}{J_m(k_0 b)} + j\sqrt{\varepsilon_r} \left[ \frac{H_{m+1}^{(2)}(kb) + \gamma^V(ka) H_{m+1}^{(1)}(kb)}{H_m^{(2)}(kb) + \gamma^V(ka) H_m^{(1)}(kb)} \right] \end{aligned} \quad (8)$$

where the denormalized  $Y_s$  is the required surface admittance for the cancellation of the  $m$ -harmonic as a function of the three main parameters of the geometry under consideration: the radius of the metal  $a$ , the relative dielectric permittivity of the substrate  $\varepsilon_r$  and the external radius  $b$ , where the admittance/impedance load is attached. Obtained inverting the  $Y_s$  value, in the next

sections the surface impedance function will be analyzed in terms of  $\omega$ -dispersion and  $m$ -harmonic cancellation.

### III. QUASI-STATIC LIMIT AND DISPERSION: COMPARISONS AND COMMENTS

Using eq. (8) for surface impedance values, the  $Z_s$  function in closed-form is of the kind

$$Z_s = R_s + jX_s = g(a, b, \varepsilon_r, m, 2\pi f) \quad (9)$$

It depends not only from geometrical and physical parameters ( $a, b, \varepsilon_r$ ), related to the specific cancellation of the harmonic ( $m$ ), but also exhibits dispersion ( $\omega = 2\pi f$ ). As reported for example in Fig. 3, the surface impedance, needed for cancellation effects, appears to be purely reactive. However, it was demonstrated by Foster [14] that, no matter how complex a reactance network is, the dispersion behaviour of lossless impedance systems is always obeying to the law

$$\frac{\partial X_s(\omega)}{\partial \omega} > 0 \quad (10)$$

which states that pure imaginary  $Z_s(\omega) = jX_s(\omega)$  must monotonically increase as a function of the frequency. As reported in Fig. 3, unfortunately this is not the case for  $X_s(\omega, m = 0)$ , here intended as the surface impedance needed for the suppression of the zero order harmonic in  $\text{TM}_z$  polarization: as a consequence, narrowband operation is expected for a single homogeneous surface impedance when passive coatings are used. However, this methodology can be useful for active metasurface cloaks [17] for any  $m$  index to suppress.

The challenge of analytical formulas for  $Z_s$  has been faced by mantle cloaking [9], even if only the  $X_s^{QS}(\omega)$  (e.g.,  $\text{TM}_z$  case) is available in the literature in closed-form expression for a metallic cylinder, here reported as

$$\begin{aligned} X_s^{QS}(\omega) &= -16\mu_0\omega \frac{b(b^2 k_0^2 - 4) \log(b/a)}{(a^2 k_0^2 - 4)(256 - 4b^2 - k_0^2 + b^6 k_0^6)} \\ &\quad \times [4(a^2 - b^2)k_0^2 + (a^2 k_0^2 - 4)(b^2 k_0^2 - 4)] \end{aligned} \quad (11)$$

and, for sake of comparison, plotted in Fig. 3. Authors in [9] have found eq. (11) for  $\text{TM}_z$  case by expanding in Taylor's series Bessel and Hankel functions involved in the overall scattering process as in Mie Theory analysis, whereas they do not report the complete formula for  $\text{TE}_z$  case because they admit that the expression appears to be cumbersome [9].

Once showing the methodology for  $\text{TM}_z$  polarization and applying duality method to derive  $\text{TE}_z$  case [12], eq. (8) offers the possibility to investigate higher order harmonics with an useful map of the  $m^{\text{th}}$  surface impedance needed to match (thus, cloaking) a particular cylindrical harmonic.

Such a closed-form investigation remains possible by treating the overall scattering process without any expansion, but, when  $Z_s$  cloaks are involved, modeling the phenomenon in terms of voltage and current waves. The expansion in Taylor's series of Bessel and Hankel functions,

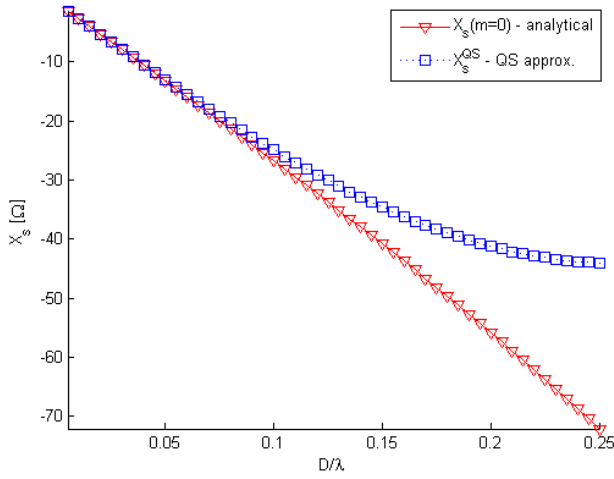


Fig. 3. Dispersion of  $X_s(\omega)$  as a function of  $D/\lambda$  (linear scale): reactance for mantle cloaking (MC) [9]  $X_s^{QS}(\omega)$  (blue square dots) and for exact analytical solution  $X_s(\omega, m=0)$  (red triangle dots).

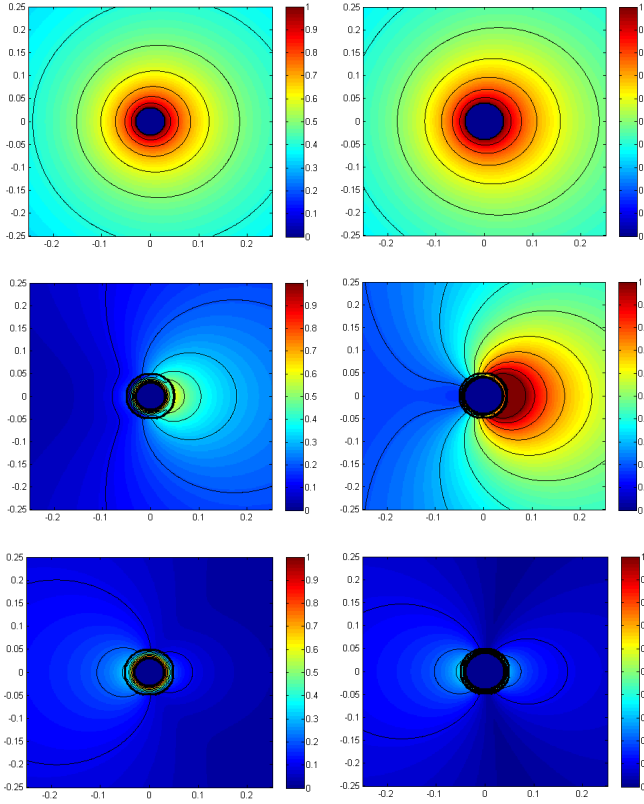


Fig. 4. Numerical results with Mie Theory (full) [8] for the absolute value (linear scale) of scattered field  $E_s$  ( $D = 0.1\lambda$ ) by changing  $a = 0.03\lambda$  (left column) and  $a = 0.04\lambda$  (right column): uncloaked case (top), cloaked case with  $X_s^{QS}$  (middle) and cloaked case with exact  $X_s(m=0)$  (bottom). Note that field contour level is set for all three cases to the same step  $\Delta|E_s| = 0.1$  V/m.

as written in [9], is consistent with the full analytical characterization found in this work: Bessel functions are addressed as the first term in eq. (8), because they refer to

the complete free-space cylindrical background in eq. (4), whereas Hankel functions appear as the second term in eq. (8), because they are compactly taken into account by the short circuit transportation through the homogeneous dielectric coating in eq. (7). Even if both curves are quite superimposed in quasi-static regime up to  $D < 0.1\lambda$ , as the device starts increasing in terms of wavelength, the gap between  $X_s^{QS}(\omega)$  and  $X_s(\omega, m=0)$  starts increasing for the same physical and geometrical structure. In order to improve the cloaking performance with exact surface impedance solutions, the graph in Fig. 3 has been exploited as a design tool: the impedance coating has been computed for a metallic cylinder of two different radii ( $a = 0.03\lambda$  and  $a = 0.04\lambda$ ), covered by an air layer at a fixed radial distance  $b = 0.05\lambda$ . For the bare metallic cylinder with  $a = 0.03\lambda$ , the quasi-static formula gives  $X_s^{QS} = -56.62 \Omega$  whereas the exact solution for the mode  $m=0$  gives  $X_s(m=0) = -62.52 \Omega$ . For the uncloaked case with  $a = 0.04\lambda$ , the quasi-static formula gives  $X_s^{QS} = -24.91 \Omega$  whereas the exact solution for the mode  $m=0$  gives  $X_s(m=0) = -26.77 \Omega$ . The surface impedance values, obtained inverting eq. (8) and from mantle cloaking via eq. (11), as reported in Fig. 3, are plotted as a function of the maximum dimension of the cloaking system in terms of wavelength (i.e.,  $D/\lambda = 2b/\lambda$ ), where the cloak is placed at  $b = 1.25a$  with a dielectric layer made of air (i.e.,  $k = k_0$ ).

In order to check the validity of the synthesis process in comparison with the quasi-static formula, a Mie Theory analysis is performed for cloaking metallic scatterers as detailed in [8]. As reported in Fig. 4, even if such case is at the border of the quasi-static condition (external diameter fixed at  $D = 0.1\lambda$ ) and thus the reactance value differs only of few  $\Omega$  in this frequency regime, the absolute value of the scattered field is different for the two cloaked cases (quasi-static and exact formula) and also when the radius  $a$  changes. With respect to the bare metallic cylinder (top), a residual scattering in the forward direction is always observed in the cloaked case according to the quasi-static formula (and even deteriorates when  $a = 0.04\lambda$ ). However, when the exact solution is employed, a deep reduction in the outside region is always observed: as a comparison, contour field level are inserted and set for all three cases to be equal with the same step  $\Delta|E_s| = 0.1$  V/m.

As it will be shown in the next section, beyond the quasi-static limit, the exact solution can serve as powerful tool for designing the dispersion of surface impedance cloaks with both Foster or Non-Foster behaviour.

#### IV. BEYOND QUASI-STATIC REGIME: ANALYTICAL DISPERSION CLOAKS WITH FOSTER/NON-FOSTER LOAD

Once chosen the geometrical and physical parameter of the geometry under investigation (i.e., radius  $a$ , substrate thickness  $\delta = b - a$  and permittivity  $\epsilon_r$ ), it is possible to consider the surface impedance values for which the cancellation of the  $m^{th}$  mode is achieved with complete dispersion dependence according to eq. (8). In this section, the geometry under investigation will be a metallic cylinder of radius  $a = 3.75$  mm, coated with a dielectric ring



of external radius  $b = 5$  mm and  $\varepsilon_r = 2.3$  for substrate permittivity: this setup is intentionally the same as the cloaked cylinder presented in [15]. The design frequency is chosen to be  $f^* = 9$  GHz, where now  $D = 0.3\lambda$  and quasi-static condition is no longer valid. In order to exploit the novel strategy based on the zero contrast approach in eq. (8), two different dispersive impedance loads are here proposed, according to the above discussion on the role played by Foster theorem [14].

One of the possible analytical solutions can follow in frequency the behaviour of a scattering mode for a fixed  $m = n$ , as

$$Z_s^{NF}(\omega) = \frac{Z_B}{\tilde{Y}_s(\omega, m = n)} \quad (12)$$

where  $n$  is the chosen harmonic index and  $Z_B = \sqrt{\mu_b/\varepsilon_b}$  is the impedance used for the denormalization (in all this study, the background is assumed to be free-space, thus  $Z_B = 120\pi \Omega$ ). A practical example of this realization to highlight the Non-Foster dispersion feature is the insertion of an active load at the surface of the cloak, such as a negative impedance converter [17]. By looking at the surface impedances given by eq. (8) for  $m = n$  with  $n = 0, 1, 2, 3$ , the choice has been considering to follow the harmonic index  $n = 1$  in this particular frequency regime: the exact solution for this geometry gives  $X_s(m = 1) = -j111.3 \Omega$  at  $f^* = 9$  GHz.

Another solution can be considering as known the dispersion function to be  $g(\omega) = 1/\omega$  around a frequency of interest and evaluate the surface impedance as

$$Z_s^F(\omega) = -j \frac{Z_B}{\omega C_{opt}} \quad (13)$$

where  $|C_{opt}| > 0$  is the value of an ideal dispersionless capacitance for which  $Z_s^F(\omega^*) = Z_s^{NF}(\omega^*, m = n)$  at the central frequency value  $\omega^* = 2\pi f^*$ . It is worthwhile mentioning that the apices in eq. (12) and eq. (13) refers to Non-Foster (NF) and Foster (F) behaviour, respectively, for both impedance loads and this affects the overall cloaking performances in the frequency band of interest.

The dispersive behaviour is shown in Fig. 5, where eq. (12) and eq. (13) have been drawn for the case of interest: by construction, their dispersion curves share the same reactance value at the frequency of interest  $f^* = 9$  GHz. The Scattering Cross Section (SCS) of the overall cylindrical system, defined as (e.g., [17]),

$$\text{SCS}(\omega) = \sum_{m=0}^{+\infty} (2 - \delta_{m,m}) |c_n^{TM}(\omega)|^2 \quad (14)$$

where  $\delta_{m,m}$  is the Kronecker delta and  $c_n^{TM(\cdot)}$  are the scattering coefficients from Mie theory [8], is here evaluated in frequency as a function of the two different impedance coatings. It is worthwhile mentioning that, negative and positive cylindrical harmonics gives the same contribution to the overall SCS, thus in eq. (14) the contribution can be evaluated as doubled for  $m = [1, +\infty)$  while a single contribution comes from the mode  $m = 0$ . As a consequence,

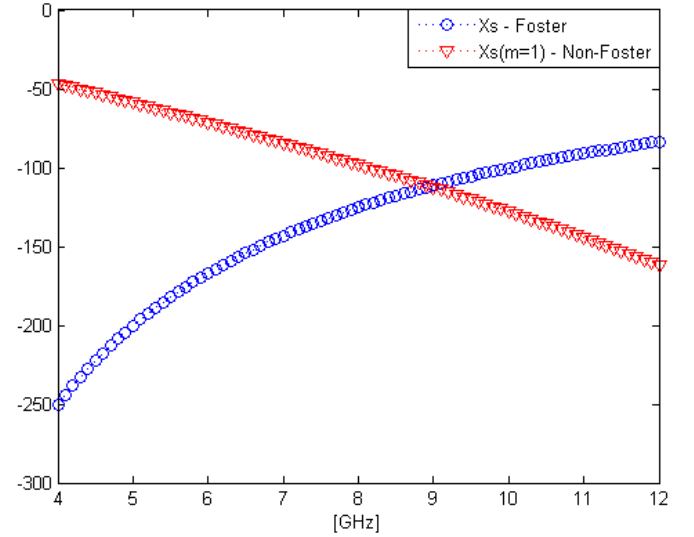


Fig. 5. Dispersion of reactances (linear scale): Foster type  $X_s^F(\omega)$  (blue points curve) and Non-Foster behaviour  $X_s^{NF}(\omega)$  (red triangle curve). Both are considered in the optimal condition at  $f^* = 9$  GHz.

the same impedance value is able to suppress both negative and positive contribution simultaneously and this is tacitly assumed for  $m = \pm 1$  (and so on) as  $m = 1$  (and so on). For sake of comparison, the Mie theory analysis as shown in [8] is performed for both uncloaked and cloaked cases (Foster and Non-Foster load) and reported in Fig. 6. With respect

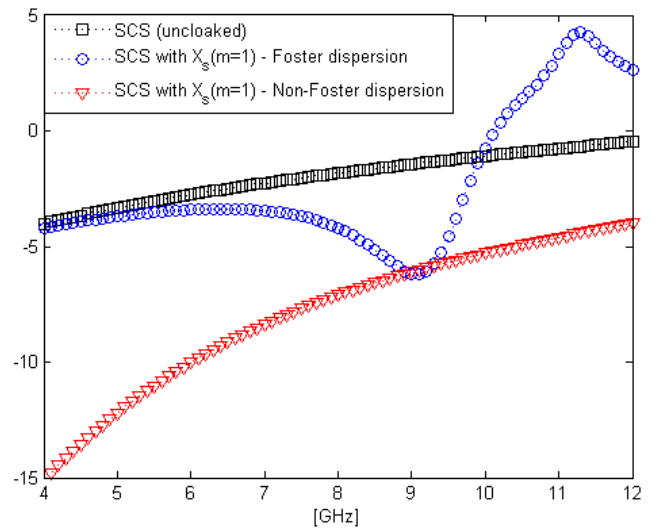


Fig. 6. SCS (dB scale) for uncloaked metallic case (black square curve) and surface impedance loads: Foster type  $X_s^F(\omega)$  (blue points curve) and Non-Foster behaviour  $X_s^{NF}(\omega)$  (red triangle curve). Both have a minimum at  $f^* = 9$  GHz, where the reactances assume by construction the same value.

to the uncloaked case (black square line), both SCS are at the minimum value at the frequency of interest: the Non-Foster coating, as expected from the main findings even for dielectric cylinders [17], shows a much wider bandwidth, especially in all the lower frequencies where the Foster

impedance load is very close to the uncloaked case.

In particular, at the frequency of interest  $f^* = 9$  GHz, the absolute value of the scattered field is reported only for the two main harmonic contribution at  $m = 0$  and  $m = 1$  in Fig. 7. Concerning the harmonic mode with

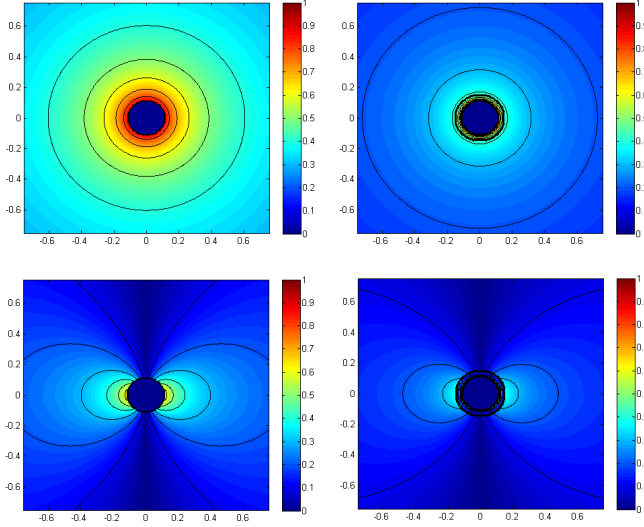


Fig. 7. Numerical results with Mie Theory (single harmonic) [8]. Specific harmonic content for the absolute value (linear scale) of scattered field  $E_s(m)$  ( $D = 0.3\lambda$  at 9 GHz) for uncloaked (left column) and cloaked case (right column): harmonic content  $|E_s|$  for  $m = 0$  (first row) and  $|E_s|$  for  $m = 1$  (second row).

$m = 0$ , which is an isotropic scattering term in 2D, the reactance value is able to cancel it with respect to the uncloaked case: at the same time, with this impedance load, the mode  $m = 1$  shows a reduced scattering contribution as expected. By choosing to follow exactly one cylindrical mode in frequency, this ensure a good performance even far from the nominal frequency  $f^*$  in terms of SCS, due to the fact that, for this particular geometry, also the lower harmonic (e.g.,  $m = 0$ ) achieves quite good suppression ensuring a  $-9$  dB reduction at the frequency  $f^*$  and an almost constant cloaking reduction from  $-11$  to  $-5$  dB suppression in the range 4 to 12 GHz with a single impedance sheet cloak.

## CONCLUSIONS AND FUTURE WORK

A novel methodology based on the zero contrast approach has been proposed as a straightforward tool for mapping surface impedance values into exact harmonic cancellation index  $m \geq 0$ , as a function of the frequency. In order to check the validity in the literature, the mantle cloaking formula [9] is confirmed in the quasi-static regime for  $m = 0$  and improved beyond the quasi-static limit. In addition, the single harmonic control with a single impedance sheet has been suggested with Foster or Non-Foster design, based on the same analytical results: (i) assuming to follow in frequency a certain mode to be cancelled (e.g.,  $m = 1$ ) with a Non-Foster load or (ii) to ensure the same amount of reduction only in a single

frequency point but with a Foster dispersion. The physical mechanism, validated through Mie theory, shows a good control of both mode  $m = 0$  and  $m = 1$ . The full potentialities of this complete mathematical theory can also be useful for the synthesis of more complicated modulation schemes for passive impedance cloaks (e.g., multilayer structures or azimuthally-smooth varying impedance profiles in microstrip-line based metasurfaces [15]), radial impedance modeling and control in leaky wave antennas [16] and novel design equations for active metasurfaces loaded with Non-Foster elements [17].

## REFERENCES

- [1] A. Alù, N. Engheta, "Achieving transparency with plasmonic and metamaterial coatings", *Phys. Rev. E*, Vol. 72, Issue 1, Article 16623, 9 pp., 2005.
- [2] U. Leonhardt, "Optical Conformal Mapping", *Science*, Vol. 312, no. 781, pp. 1777-1780, 2006.
- [3] J. B. Pendry, D. Schurig, D. R. Smith, "Controlling Electromagnetic Fields", *Science*, Vol. 312, pp. 1780-1782, 2006.
- [4] A. Alù, "Mantle cloak: Invisibility induced by a surface", *Phys. Rev. B*, Vol. 80, 245115, 2009.
- [5] P.-Y. Chen, A. Alù, "Mantle cloaking using thin patterned metasurfaces", *Physical review B*, Vol. 84, 205110, 2011.
- [6] P. Alitalo, O. Luukkonen, L. Jylha, J. Venermo, S. A. Tretyakov, "Transmission-Line Networks Cloaking Objects From Electromagnetic Fields", *IEEE Trans. on Antennas and Propagation*, vol. 56, no. 2, pp. 416-424, Feb. 2008.
- [7] P. Alitalo, A. E. Culhaoglu, A. V. Osipov, S. Thurner, E. Kemptner, S. A. Tretyakov, "Experimental Characterization of a Broadband Transmission-Line Cloak in Free Space", *IEEE Transactions on Antennas and Propagation*, vol. 60, no. 10, pp. 4963-4968, Oct. 2012.
- [8] S. Liu, H.-X. Xu, H. C. Zhang, T. J. Cui, "Tunable ultrathin mantle cloak via varactor-diode-loaded metasurface", *Optics Express*, Vol. 22, No. 11, 2014.
- [9] A. Monti, J. C. Soric, A. Alù, A. Toscano, F. Bilotti, "Anisotropic Mantle Cloaks for TM and TE Scattering Reduction", *IEEE Trans. on Antennas and Propagation*, Vol. 63, No. 4, 2015.
- [10] G. Labate, L. Matekovits, "Invisibility and cloaking structures as weak or strong solutions of Devaney-Wolf theorem", *Optics Express*, Vol. 24, No. 17, pp. 19245-19253, 2016.
- [11] G. Labate, L. Matekovits, "Kirchhoff's current law as local cloaking condition: theory and applications", *Electronics Letters*, Vol. 52, No. 21, pp. 1749-1751, 2016.
- [12] N. Marcuvitz, *Waveguide Handbook*, Electromagnetic Wave Series 21, IET, 1986.
- [13] J. -C. Sureau, "Reduction of scattering cross section of dielectric cylinder by metallic core loading", *IEEE Transactions on Antennas and Propagation*, Vol. AP-15, No. 5, 1967.
- [14] R. M. Foster, "A Reactance Theorem", *Bell System Technical Journal*, vol. 3, no. 259, 1924.
- [15] L. Matekovits, T. Bird, "Width-modulated Microstrip-line based Mantle Cloaks for Thin Single- and Multiple Cylinders", *IEEE Trans. on Antennas and Propagation*, Vol. 62, No. 5, pp. 2606 - 2615, 2014.
- [16] S. K. Podilchak, L. Matekovits, A. P. Freundorfer, Y. M. M. Antar, M. Orefice, "Controlled Leaky-Wave Radiation From a Planar Configuration of Width-Modulated Microstrip Lines", *IEEE Transactions on Antennas and Propagation*, Vol. 61, No. 10, pp. 4957-4972, 2013.
- [17] P.-Y. Chen, C. Argyropoulos, A. Alù, "Broadening the Bandwidth of Metamaterial Cloaks with Non-Foster Metasurfaces", *Phys. Rev. Lett.* 111, 233001, 2013.
- [18] N. W. McLachlan, *Bessel functions for engineers*, Oxford, Clarendon Press, p. 34, 1934.

*This work has been submitted to the IEEE for possible publication. Copyright may be transferred without notice, after which this version may no longer be accessible.*